Supporting information

Experimental section

C-doped BN nanosheet (C-BN) synthesis. The C-BN nanosheets were synthesized by plasma enhanced chemical vapor deposition (PE-CVD) in a quartz-tube reactor. The synthesis setup is shown in **Figure S1**. In detail, a gaseous triethylamine borane (TEAB, $(C_2H_5)_3N \cdot BH_3$) and ammonia were mixed as precursors for the synthesis of vertically assembled C-BN nanosheets. The partial pressure of TEAB was $1.3 \cdot 10^{-2}$ Torr. The partial pressure of ammonia was adjusted to be $1.3 \cdot 10^{-2}$, $9 \cdot 10^{-3}$ and $5.5 \cdot 10^{-3}$ Torr for the control of the carbon content in the *h*-BN lattice. Fluorine doped tin oxide (FTO) glasses (average resistivity: $7\Omega/\square$) were used as the substrates. The deposition temperature was 400°C with the radio frequency plasma power at 20 W. The powder C-BN nanosheets were synthesized through conventional annealing. The mixed precursors of boric acid, urea, and a 10 wt% of glucose were mixed, and they were annealed at 1250 °C for 8 hours. The powder is grounded and deposited on FTO glass as photoanode for measurements. Cobalt species coats on the surface of the C-BN1 for further investigation. In detail, $Co(NO_3)_2$ (1 mg) and methanol (10 ml) was as used as precursor and sacrifice agent, they are mixed in 100 ml water. The as-prepared C-BN photoanode were immersed in the solution, and the mixed system was vacuumed and illuminated by a 300 Xe light for 2 hours. The photoanode is obtained with raising by DI water.

Characterizations. The elemental composition was determined by X-ray photoelectron spectroscopy (XPS, Thermo Fisher Scientific Escalab 250Xi) and energy-dispersive X-ray spectroscopy (EDX, JEOL JSM6700 scanning electronic microscope with the EX-23000BU add-on). The sample surface was not previously treated by Ar^+ ion bombardment in XPS measurements. The types of the atom bonds in the films were determined by Fourier transform infrared (FTIR) and Raman

spectroscopies. The absorption FTIR spectra were registered within the range of 400–4000 cm^{-1} with the 2-ray SCIMITAR FTS 2000 spectrophotometer. Raman spectra were recorded on a Horiba LabRAM HR Evolution spectrometer equipped with a multichannel CCD detector cooled with liquid nitrogen ($\lambda = 632.8$ nm). The nanosheets morphology was studied using JEOL JSM6700 and Zeiss Merlin scanning electronic microscopes. Bandgap and band edges of the C-BN photoanodes were probed by ultraviolet photoelectron spectroscopy, (UPS, Thermo Fisher Scientific Escalab 250Xi instrument with He I source) and ultraviolet-visible diffusion reflector spectrometers (UV-Vis DRS, Varian Cary 500 Scan UV-visible system).

Photocatalysis measurements. Photoelectrocatalytic (PEC) measurements were conducted with a three-electrode system (BAS epsilon Electrochemical system), the CBN photoelectrodes (1 cm × 1cm), a Pt cathode and an Ag/AgCl reference electrode were used for measurement in 1.0 M NaOH electrolyte solution with an air mass 1.5 (AM 1.5) solar simulator (Newport, USA). Linear sweep voltammetry (LSV) is conducted by recording the photocurrent under AM1.5 between potentials of 0 V and 2.0 V_{RHE}. Chronoamperometry curve is conducted by recording the photocurrent with light on and off with AM 1.5 under the potential of 1.6 V_{RHE}. Triethanolamine was used in the PEC system as hole scavenge to study the efficiency of charge transfer. The electronic impedance spectroscopy (EIS) was conducted with Nyquist plots. Nyquist plots were obtained from the same system under the situations of the light on (AM 1.5) and off. Incident light-to-electron conversion efficiency (IPCE) were measured using a Xenon (300 W) with monochromator (Newport, USA). The intensity of each wavelength from the input light source was initially measured, then with the applied voltage of 1.6 V_{RHE} the photocurrent densities were measured under the certain input wavelength. Nitrogen gas was purged for 20 minutes in the PEC system prior to the

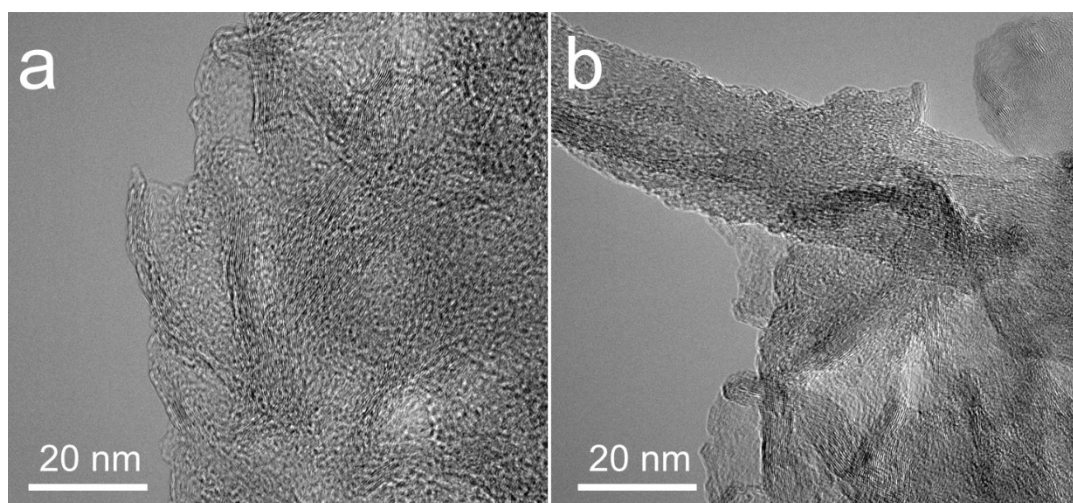photocurrent density measurements to avoid oxygen reduction reaction.
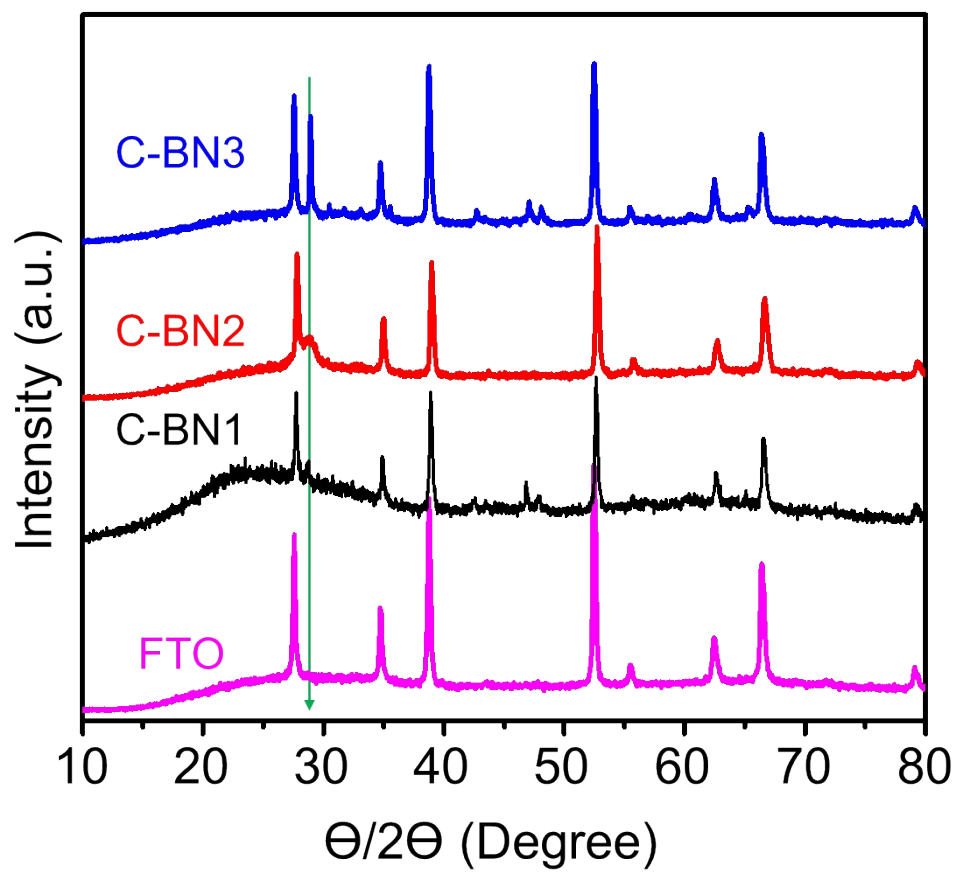
Supporting figures.
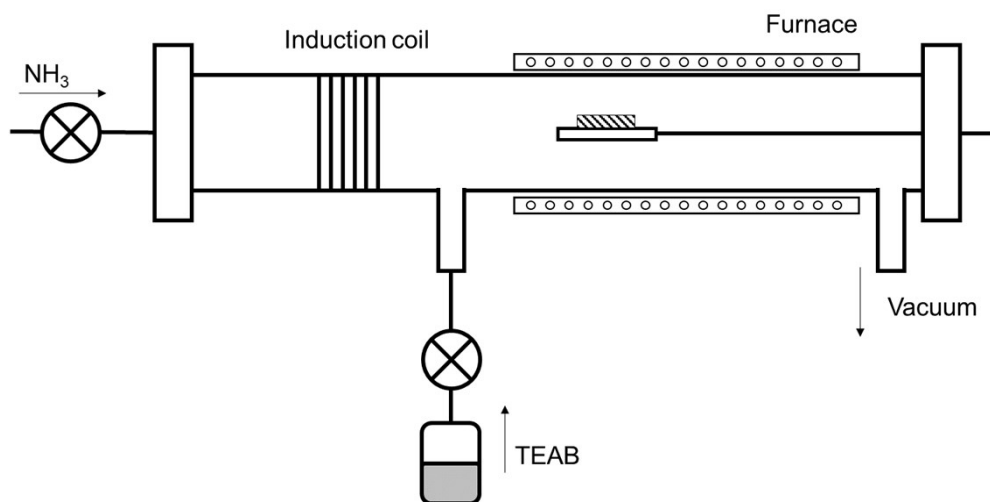
Figure S1. Schematic of the PE-CVD reactor for C-BN nanosheet synthesis.
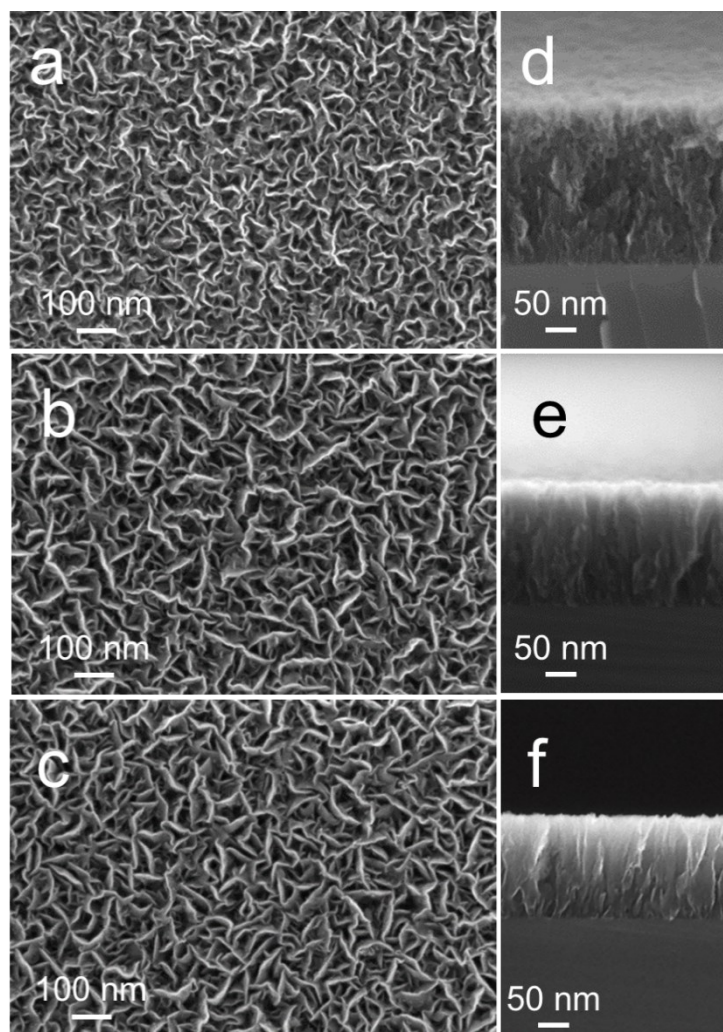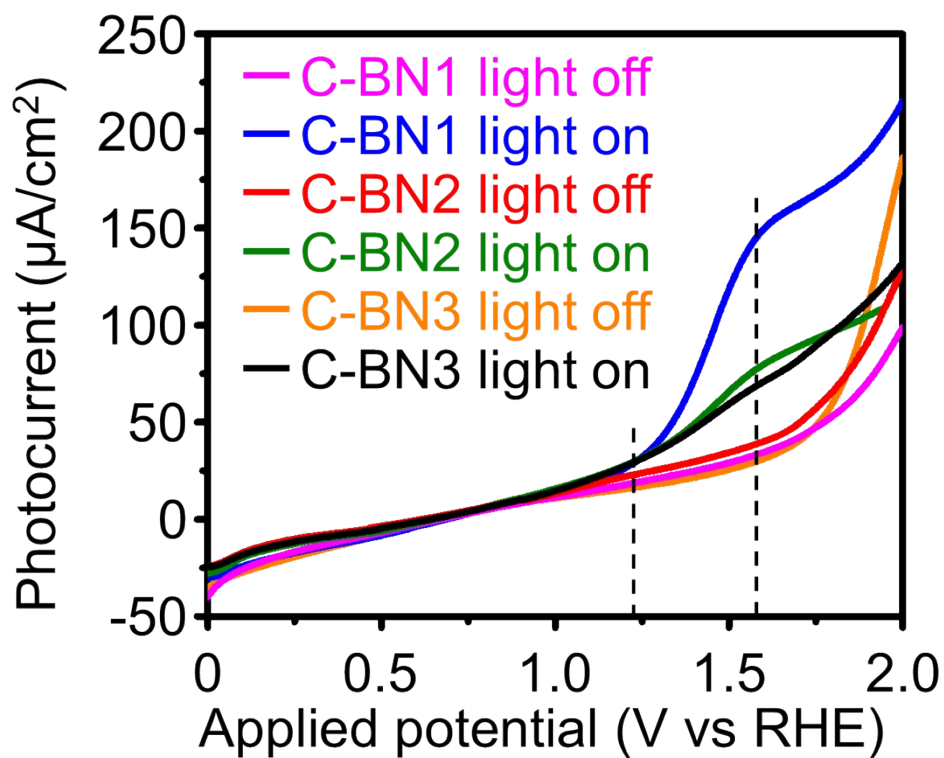
Figure. S2 SEM images of top view and cross-sectional view of the (a, d) C-BN1, (b, e) C-BN2 and (c, f) C-BN3.
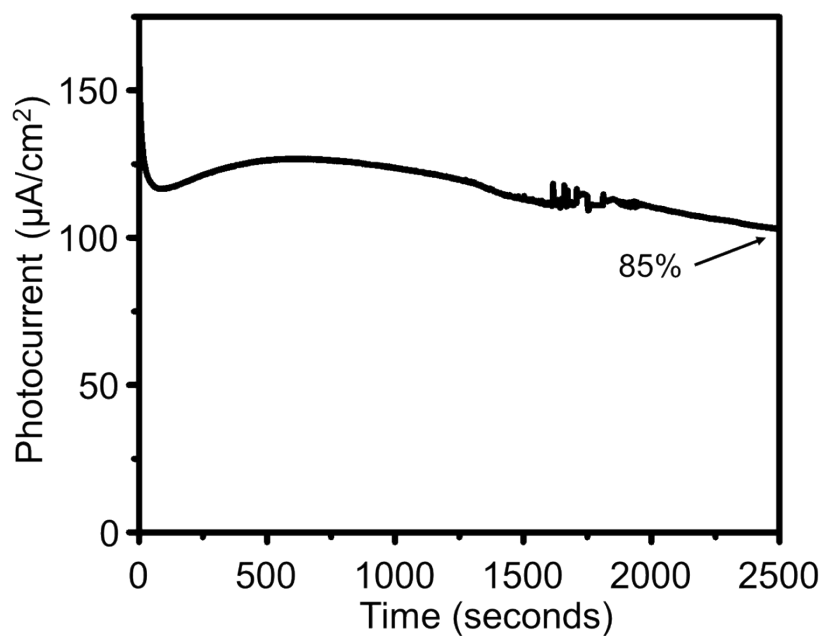

Figure S3. High resolution TEM images of C-BN, and the curvatures of the crystalline can be observed.
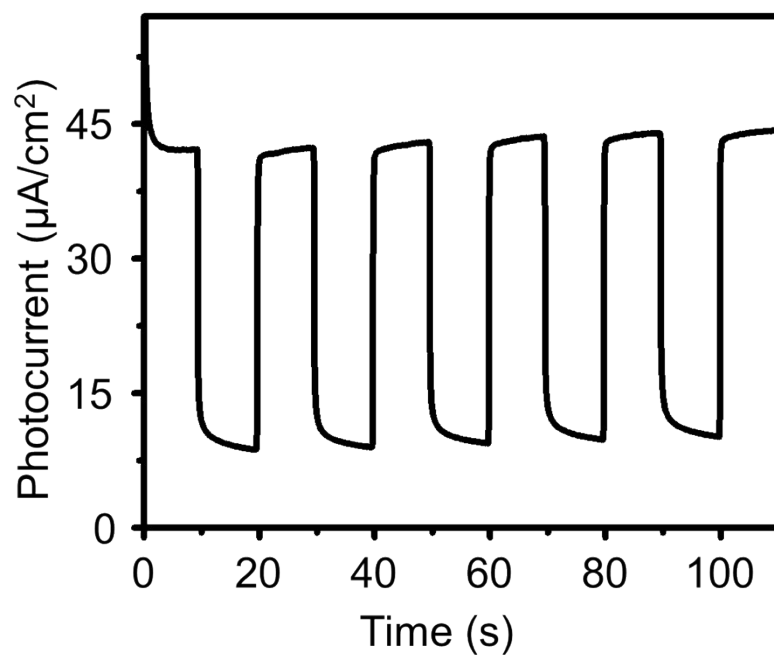
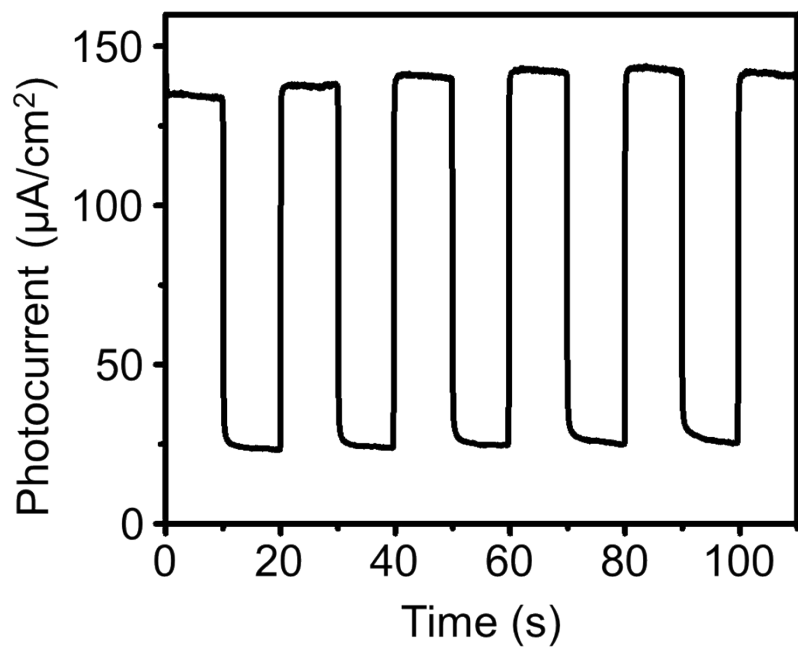**Figure S4**. XRD spectra of the FTO glass and CBN samples.

Figure S5. LSV curve shows photocurrent density with the light on and off.
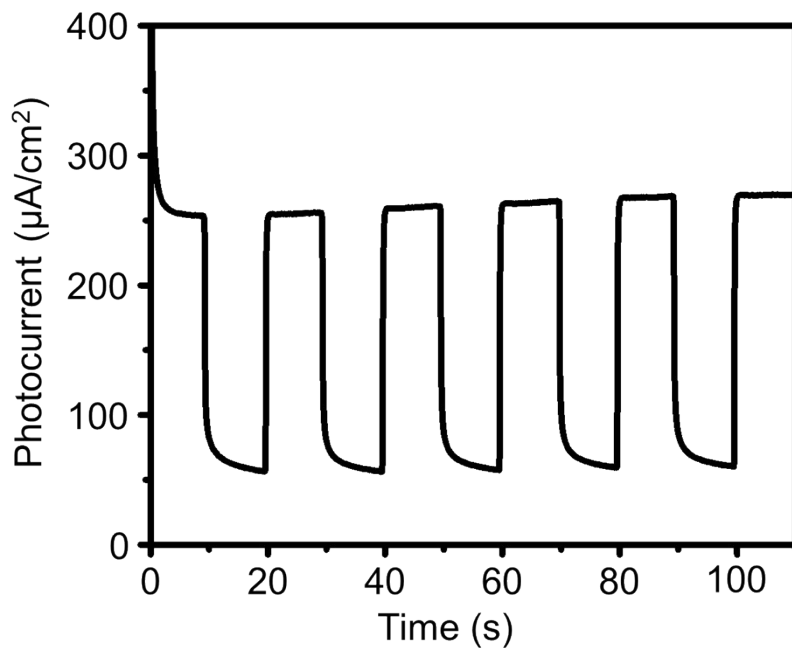

Figure S6 Long-term CA measurement, 85% photocurrent density can be preserved in the 2500 seconds.
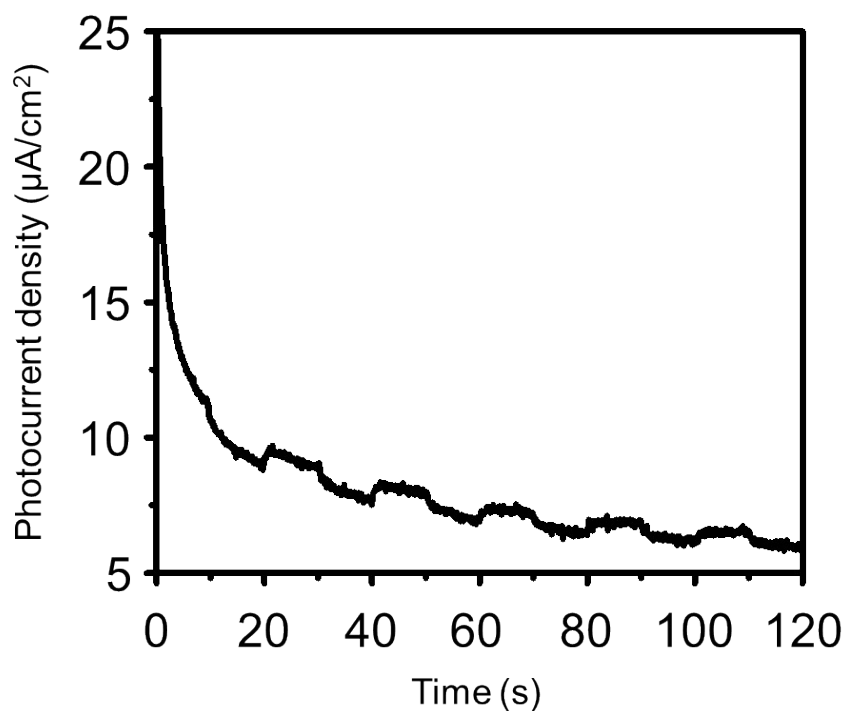
Figure S7. The photocurrent intensity of the C-BN 1 photoanode in 0.2 M Na_2SO_4 as electrolyte solution.

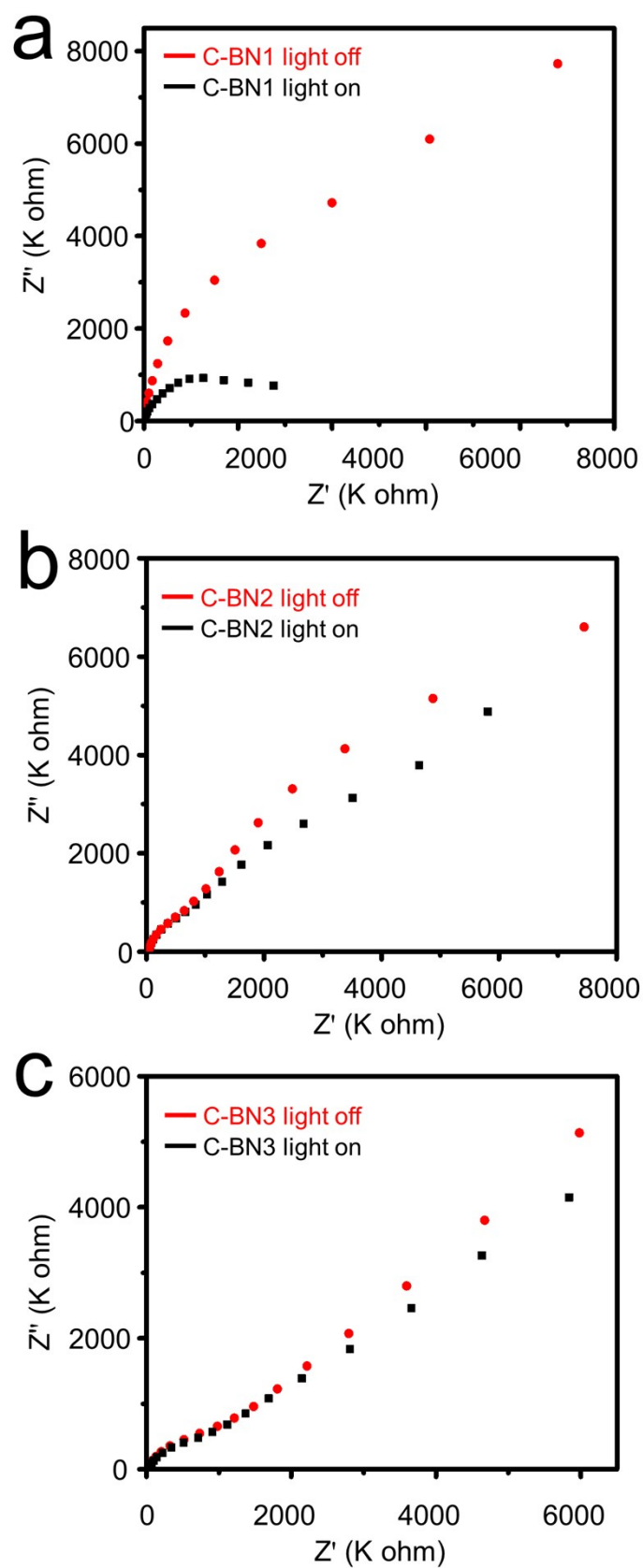**Figure S8**. The photocurrent intensity of the C-BN 1 photoanode when Co species coats on the surface.

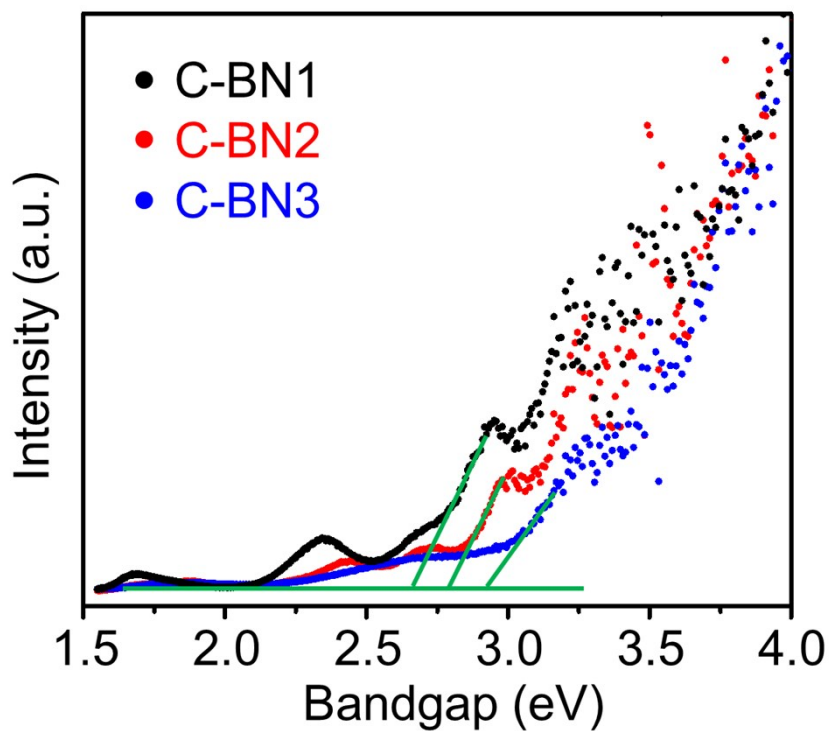**Figure S9**. The photocurrent intensity of C-BN1 by using TEOA as hole scavenge.

Figure S10. The photocurrent intensity of the powder based C-BN photoanode with 10% of carbon in the BN lattice.
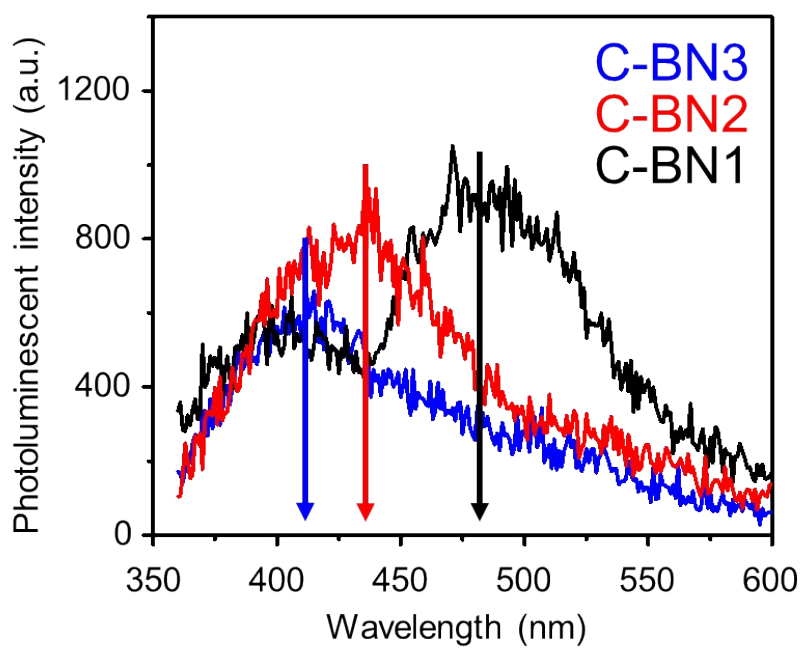
Figure S11. Nyquist plot of EIS of C-BN photoanodes with light on and off.

Figure. S12. Kubelka-Munk plots corresponds to the UV-DRS spectra of the C-BN spectra.

Figure S13. PL spectra of the CBN photoanodes.

Table S1. Comparison of the recent publications of the metal-free photoelectrode.

Material	Light source	Electrolyte solution	Potential ($\mu A\ cm^{-2}$)	ref
C-BN	AM 1.5G	1.0M NaOH	120 (1.60 V_{RHE})	This work
PCN	AM 1.5G	1.0M Na_2SO_4	100 (1.23 V_{RHE})	[1]
PCN	AM 1.5G	0.1 KOH	116 (1.23 V_{RHE})	[2]
PCN	AM 1.5G	0.1M Na_2SO_4/0.1M Na_2SO_3/0.01M Na_2SO_4	120 (1.55 V_{RHE})	[3]
PCN	AM 1.5G	0.1M Na_2SO_4	103 (1.23 V_{RHE})	[4]
3%Ni-CN	AM 1.5G	0.1 M KOH	69.8(1.23 V_{RHE})	[5]
P/B doped PCN	AM 1.5 G	0.1 M Na_2SO_4	150 ± 10(1.23 V_{RHE})	[6]
PCN nanorods	AM 1.5 G	0.1 M Na_2SO_4	120.5	[7]

*PCN=polymeric carbon nitride, *boron doped carbon nitride=BCN.

References

[1]   Y. Fang, X. Li, X. Wang, *ACS Catal.* **2018**, *8*, 8774-8780.
[2]   G. Peng, J. Albero, H. Garcia, M. Shalom, *Angew. Chem. Int. Ed.* **2018**, *57*, 15807-15811.
[3]   J. C. Bian, Q. Li, C. Huang, J. F. Li, Y. Guo, M. Zaw, R. Q. Zhang, *Nano Energy* **2015**, *15*, 353-361.
[4]   Q. S. Ruan, W. J. Luo, J. J. Xie, Y. O. Wang, X. Liu, Z. M. Bai, C. J. Carmalt, J. W. Tang, *Angew. Chem. Int. Ed.* **2017**, *56*, 8221-8225.
[5]   W. Zhang, J. Albero, L. Xi, K. M. Lange, H. Garcia, X. Wang, M. Shalom, *ACS Appl. Mater. Interfaces* **2017**, *9*, 32667-32677.
[6]   P. Luan, Q. Meng, J. Wu, Q. Li, X. Zhang, Y. Zhang, L. A. O'Dell, S. R. Raga, J. Pringle, J. C. Griffith, C. Sun, U. Bach, J. Zhang, *ChemSusChem* **2020**, *13*, 328-333.
[7]   B. Guo, L. Tian, W. Xie, A. Batool, G. Xie, Q. Xiang, S. U. Jan, R. Boddula, J. R. Gong, *Nano Lett.* **2018**, *18*, 5954-5960.